



TITLE:

# Comparison of Results from Monitoring of Bitchu-Matsuyama Castle Rock Slope and Prediction of Failure Mechanism from Numerical Model

AUTHOR(S):

GREIF, Vladimir; SASSA, Kyoji; FUKUOKA, Hiroshi

---

CITATION:

GREIF, Vladimir ...[et al]. Comparison of Results from Monitoring of Bitchu-Matsuyama Castle Rock Slope and Prediction of Failure Mechanism from Numerical Model. 京都大学防災研究所年報. B 2002, 45(B): 71-76

ISSUE DATE:

2002-04-01

URL:

<http://hdl.handle.net/2433/129089>

RIGHT:

# Comparison of Results from Monitoring of Bitchu-Matsuyama Castle Rock Slope and Prediction of Failure Mechanism from Numerical Model

GREIF Vladimir, SASSA Kyoji and FUKUOKA Hiroshi

## Synopsis

Possible rock slope failure of Bitchu-Matsuyama Castle, a cultural heritage located near Takahashi city in the central part of Okayama prefecture, is studied here. Rock mass creep movement endangers the castle, which walls are suffering damage and need to be repaired. Results from a monitoring system composed of precise extensometers and crack gauges together with thermometers and a rain gauge are presented and compared with prediction of creep movement obtained from numerical simulation. Distinct element method (DEM) model created by computer code UDEC (Universal Distinct Element Code) is used to predict catastrophic movement triggered by sliding of the toe area of the slope, suspected as most possible triggering factor of the failure of the rock slope. Both approaches are then compared and possible solutions are drawn.

**Keywords:** DEM; UDEC; rock slope monitoring; failure mechanism

## 1. Introduction

Many medieval castles build on rock substrate suffer damages both from man made and natural hazards. From the factors endangering mainly the old castles build on the rock substrate are the most common various kinds of rock movements (Vlcko J., Holzer R, 1999). In 2000 local authorities of Takahashi city came with project of safeguarding Bitchu-Matsuyama castle, which suffers damages caused by rock slope movements. Prior to maintenance or preservation works a type and size of the movement must be defined. These movements are usually determined mainly by the presence of discontinuities, which divides the rock mass into separate blocks. This feature was investigated using numerical model of rock slope, which revealed possible mechanism of failure. In the end of year 2000 started the installation of monitoring system in order to quantify the movements and determine the dangerous area. The main target was one of the defense walls close to the place where once stood the main gate.

## 2. Monitoring System

### 2.1 System of extensometers

Monitoring system in Bitchu-Matsuyama castle consists of a series of extensometers S1-S5 stretching

from the defense wall downwards to the toe slope area. Extensometers S1 and S2 are mechanical paper logging extensometers with time span of 30 days and using super invar wires to eliminate temperature effects. S1 and S2 are installed in the upper part of the rock slope, connecting the base of fortification wall with two unstable blocks in the source area of the slide.

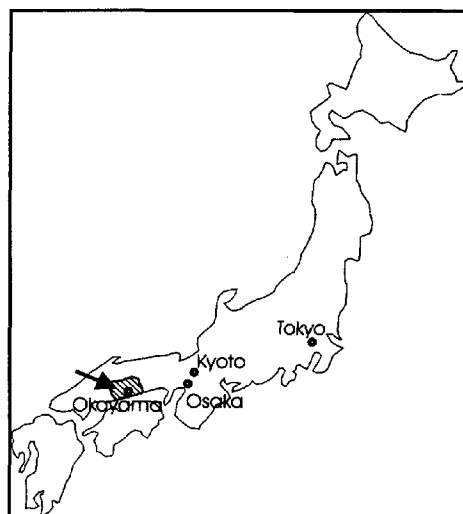


Fig.1 Location of Bitchu-Matsuyama Castle

Extensometers S3 through S5 are fully automatic extensometers working on linear variable differential transformer (LVDT) basis, which guarantees high precision of measurements about  $\pm 5.5 \times 10^{-4}$  mm. Extensometers S3 and S4 were installed to cover whole slope from the upper slope to its toe. Extensometer S5 is measuring movements of unstable tilting block in the lower part of the slope.

## 2.2 System of crack gauges

In the central part of the slope several crack gauges were set to monitor movements along these cracks. Crack gauge CRG-1 consists of two LVDT sensors to measure opening and left-right sliding of the crack, whereas crack gauge CRG-2 operating on the same basis as CRG-1 has two components as well

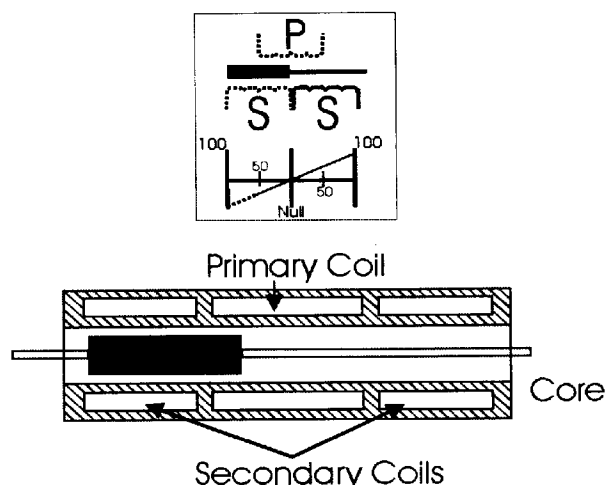


Fig. 2 Principle of LVDT measuring system

and measures forward-backward sliding and opening of the crack. Close to the crack gauge CRG-2 another LVDT sensor was set up, to investigate the temperature effect on measured displacements (Youn et al., 2002). The resolution of crack gauges is  $\pm 3 \times 10^{-4}$  mm.

## 2.3 Other monitoring devices

Beside extensometer and crack gauge systems there were installed four thermometers, three measuring temperatures near crack gauges and extensometers and one measuring temperatures approximately 10 cm inside the rock. Further an automatic rain gauge was installed in the upper part of the slope to measure precipitation.

All data from automatic devices are stored in the data logger located behind the fortification wall every 20 minutes. Figure 11 is showing the locations of monitoring devices on the face of the slope.

## 3. Monitoring Results

From late November 2000 till January 2002 many data were obtained from the monitoring devices. Few outages of electricity were caused by

lightings which were fixed later by installing a current transformer.

### 3.1 Crack gauges

The results from two crack gauges of CRG-1 are showing about 0.3 mm closing of the crack and 0.45 mm dextral sliding. The wave pattern in the opening-closing component of movement is caused by temperature effect.

The sliding component of CRG-1 suggests a downward movement of the slope situated on the right side of the monitored crack. Second crack gauge was installed on the block which was suspected to move forward from the slope face. This was however not confirmed during first year of observation and as seen from figure 4 no motion was detected in the direction of sliding component of motion and the opening component has returned back to its almost initial value forming wave with amplitude of 0.25 mm.

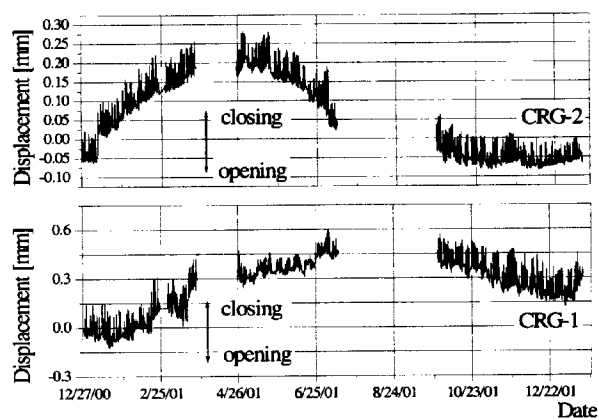


Fig. 3 Records from crack gauges CRG-1 and CRG-2 (opening-closing component)

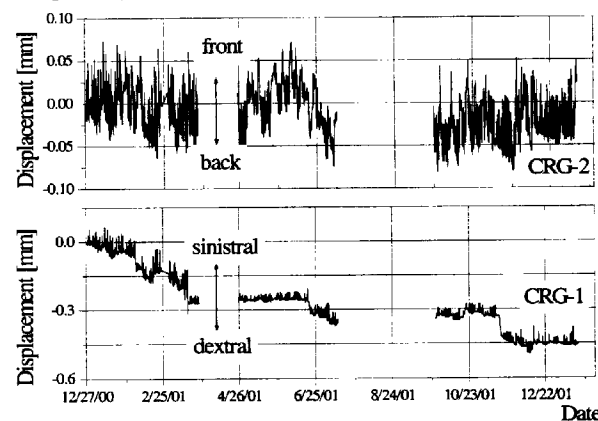


Fig. 4 Records from crack gauges CRG-1 and CRG-2 (sliding component)

The crack gauge monitoring daily and seasonal temperature changes recorded daily changes in displacement with amplitude around 0.007 mm and seasonal changes with amplitude of 0.0025 mm. By comparing these values with the amplitude of opening component of the movement it can be seen that bigger portion of the displacement is due to the

temperature effect causing volume changes of the rock rather than temperature effects on the monitoring device.

### 3.2 Extensometers

Paper extensometers S1 and S2 installed in the upper slope recorded during year 2001 compressions of 2.5mm and 6.2 mm respectively. Automatic extensometer S3 recording displacement between the base of the wall and central part o the slope measured compression about 2.57 mm and extensometer S4 extending between center of the slope and the toe has recorded compression of 3.25 mm.

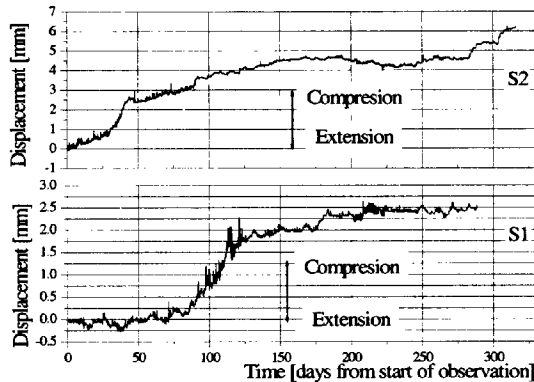


Fig. 5 Records from extensometers S1 and S2

Extensometer S5 measuring the rotational displacement of one block in the toe area recorded during four months of observation compression of 0.44 mm. This value however could be on the ascending part of a cycle thus further monitoring is necessary before drawing any conclusions.

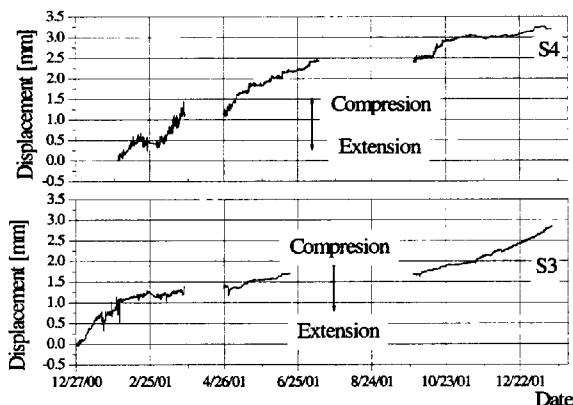


Fig. 6 Records from extensometers S3 and S4

Extensometers S1 through S4 are all exhibiting compressions which is difficult to explain by simple downward movement of the right part of the slope. It is possible that the big block which formed base for fortification wall construction is not stable and rather is moving rotationally or sliding downwards. Further monitoring and installation of another monitoring

device should prove or refute this explanation. Other explanation could possibly rely on some more complex type of movement.

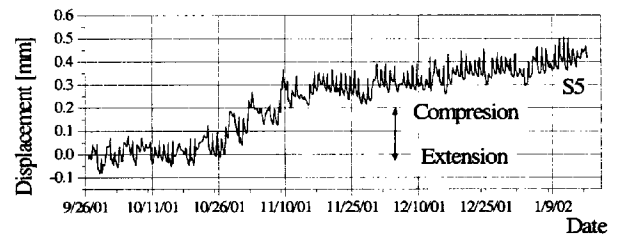


Fig. 7 Record from extensometer S5

### 3.3 Other monitoring devices

Temperatures during the year were monitored and compared with data to exclude temperature effects on monitored displacements. From the record of rain gauge can be seen that a majority of precipitation has fallen during the rainy season and following typhoon season (September – October). The cumulative precipitation for the monitored period (March 2001 – January 2002) was 1153mm.

### 4. DEM Introduction

The distinct element method introduced in 1971 by Cundall (Cundall, 1971) has found many applications in study of jointed rock masses. Different failure mechanisms were studied in both natural and artificial rock slopes. The usage of DEM attracted attention of engineers as well in problematic of slope design (Sjöberg, 1999). In the field of natural slope failure mechanism investigation the usage of DEM was focused mainly on toppling failure mechanism (Pritchard and Savigny, 1990; Deangeli and Ferrero, 2000; Pritchard and Savigny, 1991), problems of rock cliff failure (Allison and Kimber, 1998) and rock slope stability problems (Cuhan et al., 1997; Benko et al., 1994).

The essential feature of the distinct element method is its ability to model the arbitrary motion of each block with respect to any other. Block may be rigid or deformable. Because most slope stability problems involve stresses that are relatively low compared with the block strength and deformability, the blocks are usually considered rigid. The distinct element method is based on a dynamic algorithm that solves the equations of motion of the block system by an explicit finite difference method. For the analysis a distinct element code called UDEC was used.

The motion law is based on the Newton's second law of motion, which expressed in finite difference form becomes:

$$\ddot{u}_i^{(t+\Delta t/2)} = \ddot{u}_i^{(t-\Delta t/2)} + \left( \frac{\sum F_i^{(t)}}{m} + g_i \right) \Delta t \quad (1)$$

where  $\dot{u}_i$  = velocity components of block centroid

$g_i$  = gravitational acceleration components

$\Sigma F_i$  = sum of the forces acting on the block

$m$  = block mass, and

$\Delta t$  = timestep

The motion laws and joint constitutive relations are

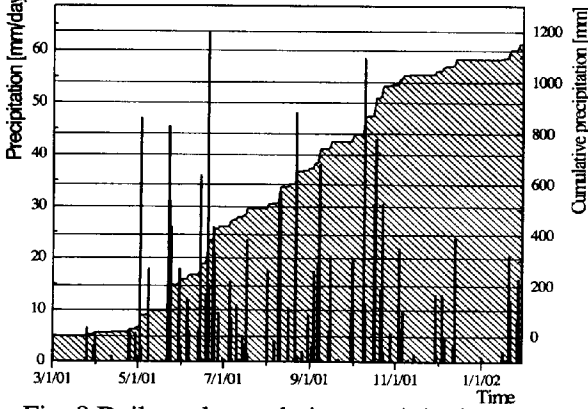


Fig. 8 Daily and cumulative precipitation during observed period

applied at each timestep. The integration of the motion law provides the new block position and joints displacement increments. Blocks are assumed to interact at discrete points referred to as “contacts” (Fairhurst C. and Lorig J. in Sharma et al., 1999).

The model geometry was created from the digital photograph oriented in direction of potential movement WSW-ENE and directions of joints were represented using automatic joint generator implemented into UDEC. The initial mechanical parameters of rock necessary for the model were found out from tests of samples taken from the rock. Some values as intact rock friction angle and joint friction angles were assumed from the properties of the similar types of rocks (Table 1). Values of normal and shear joint stiffnesses were calculated from Eq. (2) and Eq. (3) respectively with Young's modulus of rock mass assessed to be 18 GPa and joint spacing 5m.

$$k_n = \frac{E_m E_r}{s(E_r - E_m)} \quad (2)$$

$$k_s = \frac{G_m G_r}{s(G_r - G_m)} \quad (3)$$

$$G_m = \frac{E_m}{2(1 + \nu)} \quad (4)$$

where:  $k_n$  and  $k_s$  are joint normal and shear stiffnesses respectively,  $E_r$  is intact rock Young's modulus,  $G_r$  is

intact rock shear modulus,  $E_m$  is rock mass Young's modulus  $G_m$  is rock mass shear modulus,  $s$  is joint spacing and  $\nu$  is Poisson's ratio.

The rock blocks were considered to be rigid to speed up the calculation procedure. The analysis of movement mechanism was performed on the model using cell-mapping logic useful for the detection of larger relative displacements of blocks (Itasca, 1999), which reduced the calculation time necessary for the simulation. The normal joint stiffness was increased approximately two times to the value 50 GPa/m to avoid large block overlaps. The boundary conditions were applied as in Fig. 9 the left boundary was restricted from motion in X direction and the bottom boundary was immobilized in the Y direction. After applying gravitational acceleration the model was brought to equilibrium. From this point the simulation was started.

Table 1 Rock and joints properties used in UDEC

Material property	Rock	Joints
Density $\rho$ (kg/m <sup>3</sup> )	2,600	
Friction angle $\phi$ (°)	48-38	48-28
Normal stiffness $K_n$ (GPa/m)		50
Shear stiffness $K_s$ (GPa/m)		10

Considering the previous results of triggering factor analysis the toe slide seemed to be the most dangerous factor of sliding (Greif et al., 2001). In the further investigation it was necessary to find out the mechanism of the rockslide in order to be able predict the future behavior of the rock slope and optimize the monitoring system installation to find the best solution for stabilizing the slope. Therefore it was necessary to achieve longer simulation time and exaggerate the movement to be able recognize the mechanism of rock slope failure. This was done in several ways. First, the contact detection was changed to cell-mapping logic, which should secure the ability of contact tracing also with awaited larger displacements. The time step was increased to the value of  $1 \times 10^{-2}$  s, which decreased the calculation time but increased the errors as well. But for the purpose of finding out the mechanism of failure the generated errors could be neglected. Finally the joint friction angle was decreased to 5°. The triggering factor for movement was the toe slide simulated by removing one block from the toe area of slope. During the simulation three factors were monitored, namely maximal unbalanced force, joint shear displacement at five points in the slope and each 1000 calculation steps a snapshot of the model was taken in order to reveal the mechanism of failure.

By observing the simulation progress in the recorded snapshots the movement could be divided

into two phases. In the first phase the blocks were moving along planar sliding surfaces dipping in the same direction with slope face. More complex shear surface developed in the region of heavily jointed rock behind the big central block.

In the second phase the central block was subjected to toppling failure and following fall as seen in Fig.10. From the sequence is clear the damage caused to the one of the defense walls standing on the top of the slope.

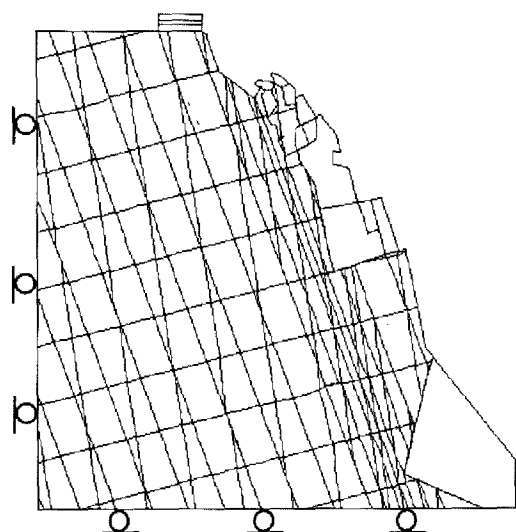


Fig. 9 Initial boundary condition used for DEM model

This type of failure is most likely the causing factor of failure of the wall, which is clear from the damage of the masonry foundation of the wall damaged by tension failure.

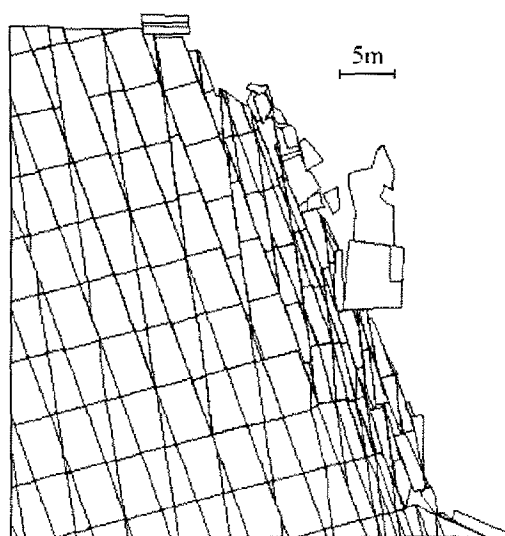


Fig. 10 Failure mechanism simulation - model after 322,000 steps

## 5. Conclusions

From the results of monitoring is clear that the slope is continual creep movement. The displacements on the cracks are rather small totally around 0.3 mm during the observation period. The extensometers are however showing considerably larger displacements in the upper part of the slope, where the erosion allows it.

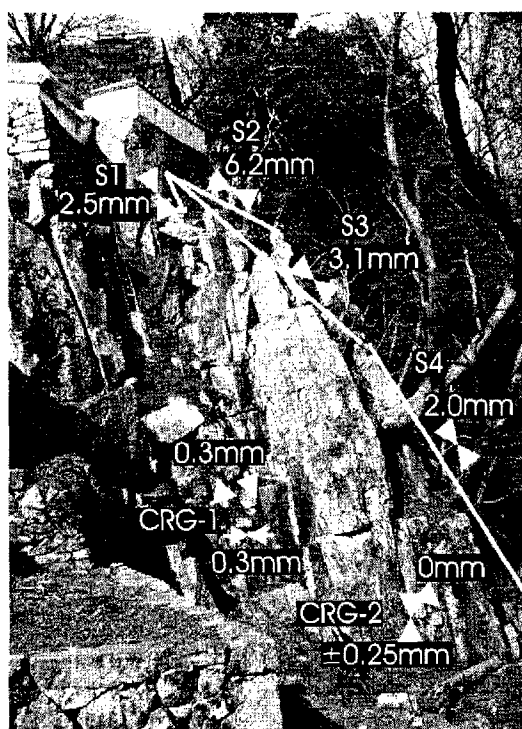


Fig. 11 Monitoring system with recorded displacements

All records from the extensometers are in compression mode which implies that the main scarp of the rock slide is located higher behind the fortification wall. Therefore the monitoring system was expanded to this area by installing bubble inclinometer fixed on the rock block forming the base of the defense wall. Further by comparison of the crack gauges CRG-2 and crack gauge monitoring temperature effects on measured displacements was found out that the temperature effect is composed from 99.1% by volume changes of the rock block induced by the seasonal changes. Only 0.16% was due to seasonal changes in the monitoring device.

The distinct element method represented by the computer code UDEC was able to recognize the mechanism of failure and greatly helped in fine-tuning the monitoring system. It correctly recognized the tension crack in the upper part of the slope, which was not observed in the field due to anthropogenic remodeling of this area.

## Acknowledgments

The research was carried out in cooperation with the Takahashi city Board of Education of Okayama

Prefecture. Mr. K. Osafune (superintendent of schools), Mr. M. Kunida and Mr. H. Mori are acknowledged for their support and cooperation. Authors want to thank to Assoc. Prof. T. Kamai and Mr. Y. Tamari for their extensive help in field investigations. Special thanks go to Mr. H. Mori for his mediatory work and his announcements without which the field study would not be possible.

## References

- Allison, R. J., Kimber, O. G. (1998): Modelling Failure Mechanisms to Explain Rock Slope Change Along the Isle of Purbeck Coast, UK. *Earth Surface Processes and Landforms*, 23, pp. 731-750
- Benko, B., Stead, D., Malgot, J. (1994): Numerical analysis of block movements as a slope failure mechanism, 7<sup>th</sup> International IAEG Congress, Balkema Rotterdam, pp.4729-4735
- Chuhan, Z., Pekau, O. A., Feng, J., Guanglun, W. (1997): Application of distinct element method in dynamic analysis of high rock slopes and blocky structures, *Soil Dynamics and Earthquake Engineering*, 16, pp. 385-394
- Cundall, P. A. (1971): A Computer Model for Simulating Progressive Large Scale Movements in Blocky Rock Systems, *Proceedings of the Symposium of the International Society of Rock Mechanics* (Nancy, France, 1971), Vol. 1, pp.132-150
- Deangeli, C., Ferrero, A. M. (2000): Rock Mechanics Studies to Analyse Toppling Failure, *Landslides in research, theory and practice*, Thomas Telford, London
- Greif, V., Sassa K., Fukuoka H. (2001): Failure and Triggering Mechanism Analysis of the Bitchu-Matsuyama Castle Rock Using Distinct Element Method, *Annals of Disas. Prev. Res. Inst., Kyoto University*, No.44 B-1, pp. 7-14
- Itasca, (1990): Udec version 3.10 – User manual, Itasca Consulting Group Inc., Minneapolis, Minnesota
- Pritchard, M. A., Savigny, K. W. (1990): Numerical modelling of toppling, *Canadian Geotechnical Journal* 27, pp. 823-834
- Pritchard, M. A., Savigny, K. W. (1991): The Heather Hill landslide: an example of large scale toppling failure in a natural slope, *Canadian Geotechnical Journal* 28, pp. 410-422
- Sharma, V. M., Saxena, K. R., Woods, R. D. (1999): Distinct Element Modelling in Geomechanics, Balkema Rotterdam, pp.220
- Sjöberg, J. (1999): Analysis of Large Scale Rock Slopes, Doctoral thesis Luleå University of Technology Sweden, pp.682
- Vlcko, J. Holzer R. (1999): Natural and Man-made Hazards Endangering the Stability of Historic Sites and Monuments in the Western Carpathians, Slovakia, *Landslide News* 12, pp. 29-34
- Youn H., Fukuoka H., Greif V. Tamari Y., Sassa K. (2002): Estimation of temperature change component in monitoring data of rock slope movement, *Inter. Symp. Landslide Risk and Mitigation and Protection of Cultural and Natural Heritage* 21.-25.January 2002, Kyoto University, Kyoto, Japan, pp.459-468

## 要旨

岡山県中部の高梁市にある文化遺産備中松山城の大手門付近の岩盤斜面が不安定化し、城壁が崩落の危機にあり、対策工による修復の必要性が検討されている。この岩盤クリープのメカニズムについて、精密伸縮計およびクラック変位計、および温度計、雨量計による観測の結果と数値シミュレーションによる予測とを比較した。また、岩盤斜面が将来崩落する場合、最も可能性の高い原因として考えられている斜面末端にある潜在地すべりにより崩落が引き起こされる過程を UDEC による離散要素法 (DEM) モデルを用いて解析し、前期の観測結果と比較検討した。

**キーワード：** 離散要素法 (DEM), UDEC, 岩盤斜面, 地すべり監視, 崩壊メカニズム